

Using spectral discretization for the
optimal \mathcal{H}_2 design of time-delay systems

*Joris Vanbiervliet,
Wim Michiels,
Elias Jarlebring*

Report TW 567, June 2010



Katholieke Universiteit Leuven
Department of Computer Science

Celestijnenlaan 200A – B-3001 Heverlee (Belgium)

Using spectral discretization for the optimal \mathcal{H}_2 design of time-delay systems

*Joris Vanbierveldt,
Wim Michiels,
Elias Jarlebring*

Report TW 567, June 2010

Department of Computer Science, K.U.Leuven

Abstract

The stabilization and robustification of a time-delay system is the topic of this paper. More precisely, we want to minimize the \mathcal{H}_2 norm of the transfer function corresponding to this class of linear time-invariant input-output systems with fixed time delays in the states. Due to the presence of the delays, the transfer function is a nonrational, nonlinear function, and the classical procedure which involves solving Lyapunov equations is no longer applicable. We therefore propose an approach based on a spectral discretization applied to a reformulation of the time-delay system as an infinite-dimensional standard linear system. In this way, we obtain a large delay-free system, which serves as an approximation to the original time-delay system, and which allows the application of standard \mathcal{H}_2 norm optimization techniques. We give an interpretation of this approach in the frequency domain and relate it to the approximation of the nonlinear terms in the time-delay transfer function by means of a rational function. Using this property, we can provide some insight in the convergence behaviour of the approximation, justifying its use for the purpose of \mathcal{H}_2 norm computation. Along with this, the easy availability of derivatives with respect to the original matrices allows for an efficient integration into any standard optimization framework. A numerical example finally illustrates how the presented method can be employed to perform optimal \mathcal{H}_2 norm design using smooth optimization techniques.

Using spectral discretization for the optimal \mathcal{H}_2 design of time-delay systems

Joris Vanbiervliet*, Wim Michiels*, Elias Jarlebring*

June 10, 2010

Abstract

The stabilization and robustification of a time-delay system is the topic of this paper. More precisely, we want to minimize the \mathcal{H}_2 norm of the transfer function corresponding to this class of linear time-invariant input-output systems with fixed time delays in the states. Due to the presence of the delays, the transfer function is a nonrational, nonlinear function, and the classical procedure which involves solving Lyapunov equations is no longer applicable. We therefore propose an approach based on a spectral discretization applied to a reformulation of the time-delay system as an infinite-dimensional standard linear system. In this way, we obtain a large delay-free system, which serves as an approximation to the original time-delay system, and which allows the application of standard \mathcal{H}_2 norm optimization techniques. We give an interpretation of this approach in the frequency domain and relate it to the approximation of the nonlinear terms in the time-delay transfer function by means of a rational function. Using this property, we can provide some insight in the convergence behaviour of the approximation, justifying its use for the purpose of \mathcal{H}_2 norm computation. Along with this, the easy availability of derivatives with respect to the original matrices allows for an efficient integration into any standard optimization framework. A numerical example finally illustrates how the presented method can be employed to perform optimal \mathcal{H}_2 norm design using smooth optimization techniques.

1 Introduction

The \mathcal{H}_2 norm is a widely known quantity associated with a linear time-invariant dynamical system. It is often used to analyze and optimize the robustness with respect to noise or external disturbances and has numerous applications in many fields of systems and control, such as performance analysis, linear quadratic regulators and optimal robust control.

The general topic of this paper is the \mathcal{H}_2 norm of time-delay systems. More precisely, we consider the system

$$\dot{x}(t) = A_0x(t) + \sum_{k=1}^m A_kx(t - \tau_k) + Bu(t), \quad (1a)$$

$$y(t) = Cx(t), \quad (1b)$$

¹Dept. of Computer Science, K.U.Leuven, Celestijnenlaan 200A, 3001 Leuven, Belgium.
E-mail: {joris.vanbiervliet, wim.michiels, elias.jarlebring}@cs.kuleuven.be

with matrices $A_0, \dots, A_m \in \mathbb{R}^{n \times n}$, $B \in \mathbb{R}^{n \times n_b}$, $C \in \mathbb{R}^{n_c \times n}$, state $x(t) \in \mathbb{R}^n$, input $u(t) \in \mathbb{R}^{n_b}$, output $y(t) \in \mathbb{R}^{n_c}$ and fixed time delays $\tau_0 < \tau_1 < \dots < \tau_m$, where $\tau_0 = 0$. In this work we will also assume that the time-delay system is stable. Note that this type of system is also known as a linear time-invariant retarded time-delay system with multiple discrete delays. See the survey paper [17] and the books [13, 15] for recent results on time-delay systems.

The \mathcal{H}_2 norm of the input-output map defined by (1), here denoted γ , is defined by

$$\gamma^2 = \|G\|_2^2 := \frac{1}{2\pi} \int_{-\infty}^{\infty} \text{tr}(G(j\omega)^* G(j\omega)) \, d\omega, \quad (2)$$

where G is the transfer function of the time-delay system,

$$G(\lambda) := C (\lambda I - \sum_{k=0}^m A_k e^{-\lambda \tau_k})^{-1} B. \quad (3)$$

Suppose A_0, \dots, A_m, B and C depend on a small number of parameters. The parameters will be considered free in the sense that they represent a parameterization of the model and often have practically meaningful interpretations, e.g., in terms of controller parameters. One possibility to assert certain properties of a model is to study how the \mathcal{H}_2 norm depends on these parameters. In particular, we often want to choose the parameters such that the \mathcal{H}_2 norm is as small as possible.

In this paper we propose a general efficient numerical scheme to compute the \mathcal{H}_2 norm of a time-delay system such that the scheme is suitable to be combined with optimization algorithms.

The method is based on discretization. The time-delay system (1) can be written as an infinite-dimensional system, which is a formulation commonly used in the field of infinite-dimensional system theory, e.g. [7]. The operator corresponding to the system is discretized and the result is a larger (standard) LTI system without delay. There are several approaches to discretize a time-delay system, e.g. with finite difference [2] or spectral collocation, employed in [5] in the context of computing characteristic roots. We will use a spectral discretization, since experience in other problems related to time-delay systems have shown attractive convergence properties. Since the discretized system is a standard LTI system, we can compute the \mathcal{H}_2 norm with standard methods. We will compute the \mathcal{H}_2 norm of the discretized system by solving a Lyapunov equation corresponding to the discretized system. The discretization method as well as the adaption of the method to the \mathcal{H}_2 norm computation is presented in Section 2.

Many general purpose optimization routines require efficient evaluation of the objective function (here γ) as well as the partial derivatives in order to work efficiently. An important advantage of the presented method is that it is constructed such that the derivatives are also cheaply available. In Section 4 we show how we can exploit the structure of the discretization in order to simplify the computation of the derivatives.

A characterization of the error in the approximation of the \mathcal{H}_2 norm is given in Section 3. It is well known that with a spectral discretization the individual characteristic roots exhibit spectral convergence, i.e., the error is $\mathcal{O}(N^{-N})$, with N the number of discretization points. This type of convergence is not expected for the \mathcal{H}_2 norm, since the latter is related to the global behaviour

of the transfer function, not the behaviour at a particular frequency. We completely characterize the convergence of the \mathcal{H}_2 norm approximation. We observe that the mid-frequency range is the main contribution of the total error of the \mathcal{H}_2 norm and that the error is of cubic order $\mathcal{O}(N^{-3})$.

There are other methods to compute the \mathcal{H}_2 norm of a time-delay system. The method in [12] is an explicit exact formula involving the solution of a so-called delay Lyapunov equation. Note that the computationally dominating part of the approach we will present here is the solving of a standard Lyapunov equation. There are numerous efficient methods to solve the standard Lyapunov equation, e.g. [1, 10, 11, 18, 3]. This is entirely different from the current situation for the delay Lyapunov equation, where not many numerical methods are available. The existing methods also tend to scale badly with respect to n for the general case.

Apart from the description of the computational scheme (Section 2) the error analysis (Section 3) and the optimization adaptations (Section 4) we also illustrate the method with examples. This is presented in Section 5. An application example stemming from the control of a heat exchange system will illustrate both the discretization approach itself as well its use in the framework of \mathcal{H}_2 norm optimization.

2 Computing the \mathcal{H}_2 norm

Computing the \mathcal{H}_2 norm of a standard LTI system (without delay) is a classical problem in systems and control and can be reformulated into solving a Lyapunov equation (see e.g. [8] or [21, Lemma 4.6]). The approach we now wish to present is based on approximating the time-delay system by a standard LTI system.

First, we will review how a time-delay system can be reformulated as a standard first order system, based on operators acting on an infinite-dimensional state. Then (in Section 2.2) we construct an approximation of the original time-delay system by replacing this state with a finite-dimensional discrete representative. This approximate system will have a larger dimension than the original dimension, but it will no longer have time delays, and its \mathcal{H}_2 norm can consequently be computed using standard methods.

2.1 Reformulation in a first order form

A time-delay system such as (1) has in a sense an infinite-dimensional character. One of the reasons for this is the fact that, instead of a mere starting point $x(0)$, also a function defined on the interval $[-\tau_m, 0]$ is required as a starting condition for the solution to be uniquely specified. This observation already led to the abstract representation in [9], involving the definition of the infinitesimal generator of the solution operator for a system of DDEs. We will present here a similar abstract representation that is more suitable in the context of input-output systems. It is based on the book [7].

Let us again introduce the function segment $\phi_t(\theta)$ belonging to the space $\mathcal{L}_2([-\tau_m, 0], \mathbb{R}^n)$ of all Lebesgue measurable functions mapping the interval $[-\tau_m, 0]$ onto \mathbb{R}^n . This function segment behaves as a sliding window that delimits the solution of the time-delay system from time $t - \tau_m$ to time t :

$$\phi_t(\theta) = x(t + \theta), \quad -\tau_m \leq \theta < 0.$$

Consider the space of all tuples that consist of on the one hand a function segment $\phi(\theta)$, and on the other hand an real, n -valued point r , or in short, $(\mathcal{L}_2([- \tau_m, 0], \mathbb{R}^n) \oplus \mathbb{R}^n)$. Let us denote this space by \mathcal{X} . We then constitute an operator \mathcal{A} whose domain is restricted to those members of \mathcal{X} satisfying the following two conditions: the function segment $\phi(\theta)$ should be absolutely continuous and differentiable on $[- \tau_m, 0]$, and r should equal the endpoint of $\phi(\theta)$, that is,

$$D(\mathcal{A}) := \left\{ \begin{pmatrix} \phi(\theta) \\ r \end{pmatrix} \in \mathcal{X} \mid \begin{array}{l} \phi \in C([- \tau_m, 0], \mathbb{R}^n) \subset \mathcal{L}_2([- \tau_m, 0], \mathbb{R}^n) \\ r = \phi(0) \end{array} \right\}. \quad (4)$$

By these two conditions, we can view a member of $D(\mathcal{A})$ as being made up of a tail $\phi(\theta)$, containing the past trajectory of the time-delay systems, and a head r , representing its present value. We can then define the action of \mathcal{A} such that it mimicks the behaviour of the time-delay system. In particular, \mathcal{A} acts on $\xi \in \mathcal{X}$ by differentiating the function segment $\phi(\theta)$, and imposing the time-delay equation on r , thereby using the function segment $\phi(\theta)$ to retrieve past information:

$$\mathcal{A}\xi = \mathcal{A} \begin{pmatrix} \phi(\theta) \\ r \end{pmatrix} := \begin{pmatrix} \phi'(\theta) \\ \sum_{k=0}^m A_k \phi(-\tau_k) \end{pmatrix}. \quad (5)$$

Similarly, we define $\mathcal{B} : \mathbb{R}^{n_w} \mapsto \mathcal{X}$ as the operator spanning r onto $\begin{pmatrix} 0 \\ Br \end{pmatrix}$, and $\mathcal{C} : \mathcal{X} \mapsto \mathbb{R}^{n_z}$ as the operator mapping $\begin{pmatrix} \phi(\theta) \\ r \end{pmatrix}$ onto Cr .

With these three operators, and using $\xi \in \mathcal{X}$ as the new state, we can write the time-delay system (1) in the following format

$$\frac{d}{dt}\xi(t) = \mathcal{A}\xi(t) + \mathcal{B}w(t), \quad (6a)$$

$$z(t) = \mathcal{C}\xi(t) + Dw(t). \quad (6b)$$

2.2 A spectral discretization

This section outlines the procedure to discretize the abstract system (6) into a finite-dimensional one. We adapt the same procedure that was used in [6] in order to approximate the spectrum of a time-delay system.

Consider a grid Ω_N of N distinct points in the interval $[- \tau_m, 0]$,

$$\Omega_N = \{\theta_i, \quad i = 1, \dots, N\}. \quad (7)$$

In what follows, we will fix Ω_N to the grid consisting of the N scaled and shifted Chebychev extremal points, that is,

$$\theta_{i+1} = \frac{\tau_m}{2}(\chi_i - 1), \quad i = 0, \dots, N - 1, \quad (8)$$

with χ_i defined by

$$\chi_i = \cos\left(\pi - \frac{i\pi}{N - 1}\right), \quad i = 0, \dots, N - 1 \quad (9)$$

Note that the endpoints are included in the grid, that is, $\theta_1 = - \tau_m$ and $\theta_N = 0$.

The discretization is executed by replacing the infinite-dimensional space \mathcal{X} by \mathbb{X}_N , the space of discrete functions over the mesh Ω_N . Specifically, a member $\xi = \begin{pmatrix} \phi(\theta) \\ r \end{pmatrix} \in \mathcal{X}$ is replaced by its discrete counterpart $X \in \mathbb{X}_N$, which is the $Nn \times 1$ block vector

$$X = \begin{bmatrix} X_1 \\ \vdots \\ X_N \end{bmatrix} \in \mathbb{R}^{Nn}$$

that fulfills

$$X_i = \begin{cases} \phi(\theta_i) & i = 1, \dots, N-1, \\ r & i = N. \end{cases} \quad (10)$$

Each element $X \in \mathbb{X}_N$ corresponds to a unique \mathbb{R}^n -valued degree $N-1$ polynomial $\Phi(\theta)$ that interpolates between the Nn discrete points of X . Using a Lagrangian basis, this polynomial $\Phi(\theta)$ can be represented as a linear combination with the block components of X as coefficients:

$$\Phi(\theta) = \sum_{j=1}^N X_j \ell_j(\theta), \quad \theta \in [-\tau_m, 0]. \quad (11)$$

Here, the functions $\ell_j(\theta)$, $j = 1, \dots, N$ denote the N Lagrange polynomials defined as the real-valued polynomials of degree $N-1$ that satisfy

$$\ell_j(\theta_i) = \begin{cases} 1, & i = j, \\ 0, & i \neq j, \end{cases} \quad i, j \in \{1, \dots, N\}. \quad (12)$$

Evidently, we can then write down the derivative of $\Phi(\theta)$ as

$$\Phi'(\theta) = \sum_{j=1}^N X_j \ell'_j(\theta).$$

The discrete evaluation on the mesh of this function, that is, the $Nn \times 1$ vector $\Phi'_N(\Omega_N) = [\Phi'_N(\theta_1)^\top \dots \Phi'_N(\theta_N)^\top]^\top$, can be written as a matrix vector product,

$$\Phi'_N(\Omega_N) = (D_N \otimes I_n)X. \quad (13)$$

Here, \otimes denotes the Kronecker product and $D_N \in \mathbb{R}^{N \times N}$ is the so-called differentiation matrix defined by

$$D_N(i, j) = d_{ij} = \ell'_j(\theta_i), \quad i, j \in \{1, \dots, N\}.$$

We approximate the $\mathcal{X} \rightarrow \mathcal{X}$ operator \mathcal{A} by an $\mathbb{X}_N \rightarrow \mathbb{X}_N$ operator \mathcal{A}_N , namely the N -by- N block matrix of n -by- n submatrices a_{ij} , $i, j \in \{1, \dots, N\}$,

$$\mathcal{A}_N = \begin{bmatrix} a_{11} & \dots & a_{1N} \\ \vdots & \ddots & \vdots \\ a_{N1} & \dots & a_{NN} \end{bmatrix}.$$

If we want \mathcal{A}_N to have the same effect on the interpolating polynomial $\phi(\theta)$ as \mathcal{A} has on a member of \mathcal{X} (i.e., as in (5)) in the discretization points θ_i , we must ensure that

$$\mathcal{A}_N X = \mathcal{A}_N \Phi(\Omega_N) = \left[\Phi'(\theta_1)^\top, \dots, \Phi'(\theta_{N-1})^\top, \left(\sum_{k=0}^m A_k \Phi(-\tau_k) \right)^\top \right]^\top.$$

This implies that the top $N - 1$ block row entries of \mathcal{A}_N simply equal those of the matrix $D_N \otimes I_n$, and that the original time-delay information is only contained in the bottom block row. By (13) and (11), we can write down the block entries of \mathcal{A}_N explicitly

$$a_{ij} = \begin{cases} d_{ij} I_n & j \in \{1, \dots, N\}, i \in \{1, \dots, N - 1\}, \\ \sum_{k=0}^m \ell_j(-\tau_k) A_k & j \in \{1, \dots, N\}, i = N. \end{cases} \quad (14)$$

Note that the values $\ell_j(-\tau_k)$ can be computed very efficiently using the barycentric interpolation formula, because the discretization grid Ω_N was chosen to contain the Chebychev points of the second kind (see [4]).

In the same fashion we can approximate operators \mathcal{B} and \mathcal{C} with the matrices $\mathcal{B}_N \in \mathbb{R}^{Nn \times n_w}$ and $\mathcal{C}_N \in \mathbb{R}^{n_z \times Nn}$, namely by constructing them as

$$\mathcal{B}_N = \begin{bmatrix} 0 & \cdots & 0 & I_n \end{bmatrix}^\top B \quad \text{and} \quad \mathcal{C}_N = C \begin{bmatrix} 0 & \cdots & 0 & I_n \end{bmatrix} \quad (15)$$

We now have all the ingredients to approximate the abstract system (6) with the linear system

$$X'(t) = \mathcal{A}_N X(t) + \mathcal{B}_N w(t), \quad (16a)$$

$$z(t) = \mathcal{C}_N X(t) \quad (16b)$$

Note that the dimension of this system is equal to the dimension of the original time-delay system multiplied by the number of discretization points N .

2.3 Evaluation of the \mathcal{H}_2 norm

The numerical procedure for approximating γ , the \mathcal{H}_2 norm of the time-delay system, is as follows. We discretize the time-delay system with a fixed discretization parameter N , and compute γ_N instead, namely the \mathcal{H}_2 norm based on the discretized system,

$$\gamma_N^2 := \|G_N\|_2^2 = \frac{1}{2\pi} \int_{-\infty}^{\infty} \text{tr}(G_N(j\omega)^* G_N(j\omega)) \, d\omega, \quad (17)$$

where G_N is the LTI transfer function

$$G_N(\lambda) := \mathcal{C}_N (\lambda I - \mathcal{A}_N)^{-1} \mathcal{B}_N. \quad (18)$$

Recall that for a delay-free system, such as system (16), we have the following property.

Property 2.1. *For stable or Hurwitz matrix \mathcal{A}_N , let controllability respectively observability Gramians P_N and Q_N be the unique symmetric Nn -by- Nn matrices that satisfy the following primal-dual Lyapunov equation pair*

$$\mathcal{A}_N P_N + P_N \mathcal{A}_N^\top = -\mathcal{B}_N \mathcal{B}_N^\top, \quad (19a)$$

$$\mathcal{A}_N^\top Q_N + Q_N \mathcal{A}_N = -\mathcal{C}_N^\top \mathcal{C}_N. \quad (19b)$$

Then the \mathcal{H}_2 norm of system (16), with transfer function G_N , can be computed by

$$\gamma_N^2 = \text{tr}(\mathcal{C}_N^\top P_N \mathcal{C}_N) = \text{tr}(\mathcal{B}_N Q_N \mathcal{B}_N^\top) \quad (20)$$

The Lyapunov equations (19) can be loosely regarded as discretizations of the operator-based Lyapunov equations belonging the abstract system (6).

3 Error analysis

The discretized linear system (16) is constructed such that it is an approximation of the time-delay system (1). Hence, it is to expect that γ_N , i.e., the \mathcal{H}_2 norm of the discretized linear system, will approximate γ . This is indicated by the fact that in [6], it was proven that the eigenvalues of \mathcal{A}_N exhibited a spectral convergence towards the eigenvalues of solution operator's infinitesimal generator \mathcal{A} .

In this section we will characterize how the approximation error depends on the discretization parameter N . Before doing so, we will first prove some properties for the transfer function of the discretized time-delay system $G_N(\lambda)$.

3.1 Interpretation in the frequency domain

Let us introduce a function $\hat{G}(\lambda)$ that is obtained by replacing the nonlinear exponential terms $e^{-\lambda\tau_k}$ in expression (3) for $G(\lambda)$ by the values $p_N(-\tau_k; \lambda)$. These latter are to be interpreted as the evaluations at points $t = -\tau_k$ of a collocation polynomial $p_N(t; \lambda)$ which approximates the exponential function $e^{\lambda t}$ for t in the interval $[-\tau_m, 0]$. Formally, we have the following definition.

Definition 3.1. For $\lambda \in \mathbb{C}$, let $\hat{G}_N(\lambda)$ be defined as

$$\hat{G}_N(\lambda) = C \left(\lambda I_n - \sum_{k=0}^m A_k p_N(-\tau_k; \lambda) \right)^{-1} B, \quad (21)$$

where $p_N(\cdot; \lambda)$ is the polynomial of degree $N - 1$ satisfying

$$p'_N(\theta_i; \lambda) = \lambda p_N(\theta_i; \lambda), \quad i = 1, \dots, N - 1, \quad (22)$$

$$p_N(\theta_N; \lambda) = 1. \quad (23)$$

with θ_i the elements of the grid Ω_N .

Later on in this section, we will prove that $\hat{G}(\lambda)$ is identical to the transfer function obtained by discretizing the time-delay system into the linear system (16). Let us however first look at some properties concerning the function p_N .

It is easily appreciated that the function $p_N(t; \lambda)$ is indeed a polynomial that approximates the exponential function $e^{\lambda t}$ in t on the interval $[-\tau_m, 0]$. The first $N - 1$ equations (22) are collocation conditions for the differential equation $x'(t) = \lambda x(t)$, of which $e^{\lambda t}$ is a solution, and the last equation (23) is simply an interpolation requirement at $t = 0$.

Knowing that $p_N(\cdot; \lambda)$ collocates $e^{\lambda t}$, what can we say about $p_N(-\tau_k; \cdot)$ as a function of λ ? It will turn out that $p_N(\cdot; \lambda)$ is in fact a rational approximation to $e^{\lambda t}$. To see this, let us first prove the following theorem, which gives an explicit expression for p_N .

Theorem 3.2. Let D_N^a be the upper left $(N - 1) \times (N - 1)$ square block of the differentiation matrix D_N and let D_N^b be the remaining upper right $(N - 1) \times 1$ vector that resides next to D_N^a in D_N , then the function $p_N(t; \lambda)$ can be written down explicitly as

$$p_N(t; \lambda) = [\ell_1(t) \quad \dots \quad \ell_{N-1}(t)] (\lambda I - D_N^a)^{-1} D_N^b + \ell_N(t), \quad (24)$$

where $\ell_j(t)$, $j = 1, \dots, N$ are the Lagrangian polynomials as defined in (12).

Proof. In a Lagrangian basis on the grid Ω we can express p_N as a linear combination of the function evaluations in the gridpoints

$$\begin{aligned} p_N(t; \lambda) &= \sum_{j=1}^N \ell_j(t) p_N(\theta_j, \lambda) \\ &= \begin{bmatrix} \ell_1(t) & \cdots & \ell_N(t) \end{bmatrix} \begin{bmatrix} p_N(\theta_1; \lambda) & \cdots & p_N(\theta_N; \lambda) \end{bmatrix}^\top. \end{aligned} \quad (25)$$

Note that only the second vector containing the grid evaluations $p_N(\theta_j, \lambda)$, $j = 1, \dots, N-1$, depends on λ . To find these values, we can require that the conditions (22) and (23) must hold.

Filling in the Lagrangian basis expansion, the interpolation condition (23) simply reads as $p_N(\theta_N, \lambda) = 1$. Imposing additionally the collocation conditions (22) on (25), we obtain

$$\sum_{j=1}^{N-1} \ell'_j(\theta_i) p_N(\theta_j, \lambda) + \ell'_N(\theta_i) = \lambda p_N(\theta_i, \lambda), \quad i = 1, \dots, N-1.$$

Recalling that $\ell'_j(\theta_i)$ are the elements d_{ij} of D_N , we can rewrite this in matrix-vector form as

$$(\lambda I - D_N^a) \begin{bmatrix} p_N(\theta_1; \lambda) & \cdots & p_N(\theta_{N-1}; \lambda) \end{bmatrix}^\top = D_N^b, \quad (26)$$

from which we obtain

$$\begin{bmatrix} p_N(\theta_1; \lambda) & \cdots & p_N(\theta_{N-1}; \lambda) \end{bmatrix}^\top = (\lambda I - D_N^a)^{-1} D_N^b. \quad (27)$$

Filling in in the Lagrangian basis expansion (25), together with $p_N(\theta_N, \lambda) = 1$, the assertion follows. \square

A consequence of the expression in the previous theorem is described in the following corollary, stating that the functions $\lambda \mapsto p_N(-\tau_k; \lambda)$ are proper rational functions with common poles.

Corollary 3.3. *We can express p_N as the rational function*

$$p_N(-\tau_k; \lambda) = \frac{r_k(\lambda)}{s(\lambda)}, \quad k = 1, \dots, m, \quad (28)$$

where $r_k(\lambda)$, $k = 1, \dots, m$ are polynomials of degree smaller than or equal to $N-1$, and $s(\lambda)$ is the monic polynomial of degree $N-1$ determined by

$$s(\lambda) = \det(\lambda I - D_N^a), \quad (29)$$

with D_N^a as in Theorem 3.2.

Proof. This follows directly by the fact that $(\lambda - D_N^a)^{-1}$ can be written as $\text{adj}(\lambda - D_N^a) / \det(\lambda - D_N^a)$. \square

We are now ready to state (and prove in appendix) the main result of this section. It is set out in the theorem below. The proof, which is quite technical, can be found in appendix A.

Theorem 3.4. *The transfer function $G_N(\lambda)$ of the discretized time-delay system, as defined in (18), is identical to the function $\hat{G}_N(\lambda)$, as determined in Definition 3.1,*

$$G_N(\lambda) = \hat{G}_N(\lambda).$$

Consequently, the computation of the value γ_N by formula (20) can be interpreted as the evaluation of the \mathcal{H}_2 norm corresponding to a system with transfer function equal to $\hat{G}_N(\lambda)$, i.e.,

$$\gamma_N = \|G_N\|_2 = \|\hat{G}_N\|_2.$$

This theorem gives an interpretation of the discretization strategy outlined in Section 2.2 as replacing the nonlinear exponential terms $e^{-\lambda\tau_k}$ in $G(\lambda)$ by the rational approximations $p_N(-\tau_k; \lambda)$. This connection will be essential in studying the convergence properties of this discretization approach.

3.2 Convergence properties of the \mathcal{H}_2 norm

With the interpretation of Subsection 3.1 in mind, we will now investigate the convergence properties of γ_N . The approximation error of the \mathcal{H}_2 norm can be reformulated as

$$\begin{aligned} \gamma_N^2 - \gamma^2 &= \|G_N\|_2^2 - \|G\|_2^2 \\ &= \frac{1}{2\pi} \int_{-\infty}^{\infty} \|G_N(j\omega)\|_F^2 d\omega - \frac{1}{2\pi} \int_{-\infty}^{\infty} \|G(j\omega)\|_F^2 d\omega \\ &= \frac{1}{\pi} \int_0^{\infty} (\|G_N(j\omega)\|_F - \|G(j\omega)\|_F) d\omega. \end{aligned} \quad (30)$$

Let E_N denote the corresponding point-wise error,

$$E_N(\omega) := \|G_N(j\omega)\|_F - \|G(j\omega)\|_F. \quad (31)$$

We ultimately wish to study $\gamma_N^2 - \gamma^2$ as a function of N . This is achieved by using the interpretation in the frequency domain to see how the point-wise error $E_N(\omega)$ depends on ω and N . Indeed, we can view E_N as the difference in Frobenius norms resulting from replacing the exponential terms in G by the rational approximations as presented in the previous subsection. Therefore, we will first study how the approximation by $p_N(t; \lambda)$ of the exponential function $e^{\lambda t}$ behaves as a function of λ .

3.2.1 Error behaviour of p_N

Let e_N denote the difference on the imaginary axis,

$$e_N(t; \omega) := |p_N(t; j\omega) - \exp(j\omega t)|.$$

The maximal error of p_N on the delay interval, that is, $\max_{t \in [-\tau_m, 0]} e_N(t; \omega)$, as a function of ω , is illustrated in Figure 1. The maximal delay τ_m is chosen to be equal to 1 without loss of generality, as another choice for τ_m would simply result in a scaling of the argument ω . It can be observed that the error of the approximation as a function of ω is negligible up to a certain critical value of ω , which we will denote ω_T . Beyond this critical ω_T , the error first grows

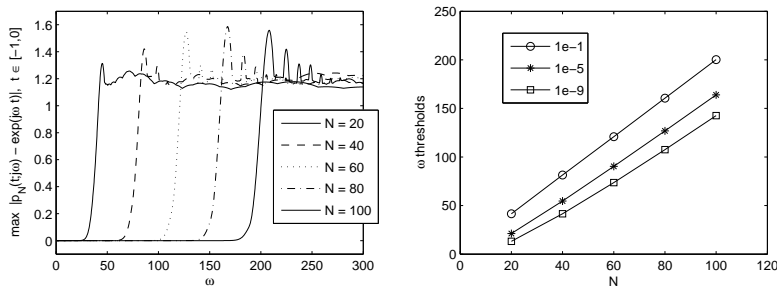


Figure 1: (Left) Maximal error between $p_N(t; j\omega)$ and $e^{-j\omega t}$ on the interval $t \in [-1, 0]$ for N values ranging between 10 and 100. (Right) Threshold ω values for various precision ($10^{-1}, 10^{-5}$ and 10^{-9}) as a function of N

exponentially to $\mathcal{O}(1)$, and then remains in this order of magnitude. The reason that e_N stays bounded for large ω , lies in the fact that p_N converges to ℓ_N for $\omega \rightarrow \infty$. This can be seen by taking the limit for λ of explicit expression (24). The ω values from which on the approximation starts breaking down seem to follow a linear increase with N . This is confirmed by the right subfigure of Fig. 1, depicting the maximal values of ω for which the error is smaller than a specific precision. Note that the characterization of e_N shown in these two figures is (apart from the scaling of τ_m) problem independent and Fig. 1 visualizes a very general result.

3.2.2 Error behaviour of G_N

With the following example we illustrate that the threshold behaviour of e_N propagates to $E_N(\omega)$.

Example 3.5. Consider the following input-output system with two delays $\tau_1 = 1$, $\tau_2 = 2$ and matrices

$$A_0 = \begin{bmatrix} 0 & 1 \\ -4 & -1 \end{bmatrix}, A_1 = \begin{bmatrix} 0 & 0 \\ 2 & 1 \end{bmatrix}, A_2 = \begin{bmatrix} 1 & 1 \\ 1 & 0 \end{bmatrix}, B = C^\top = \begin{bmatrix} 1 \\ 1 \end{bmatrix}.$$

In Figure 2, the Frobenius norm of both $G(j\omega)$ and $G_N(j\omega)$ is plotted together with e_N for a discretization value $N = 7$. We see that the value of ω_T , the ω for which the approximation by p_N breaks down and e_N starts growing, corresponds very well with the ω for which the approximation of $G_N(j\omega)$ to $G(j\omega)$ breaks down. More tests indicated that this appears to be true in general.

Note that although the reasoning is in a sense rough, it is very general. The thresholds of $e_N(\omega)$ and $E_N(\omega)$ really coincide for all the examples tested. Moreover, the function e_N is essentially problem independent. Indeed, it only depends on the maximal delay and not on the system matrices, and this dependence can be completely removed by scaling the problem in a preliminary step.

From the reasoning above, we have illustrated that there exists an asymptotically linear, increasing function $\omega_T(N)$ for which the error contribution of $E_N(\omega)$ for $\omega < \omega_T(N)$ can be neglected. For sufficiently large N , this means

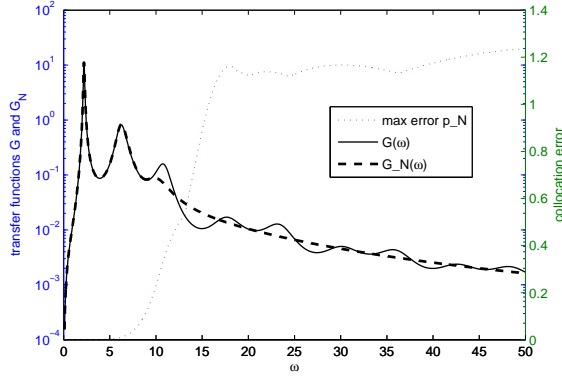


Figure 2: The Frobenius norms of the approximate transfer function G_N and the exact transfer function G for Example 3.5 and $N = 7$ in relation with the maximal collocation error of p_N (dotted line).

that the dominant part of the error stems from the high frequencies. This motivates us to investigate what happens with E_N for large ω , i.e., beyond the critical ω_T . From Figure 2, we can already see that G_N seems to have the same asymptotic behaviour as G .

To investigate this claim further, let us express the first two terms in the asymptotic expansion of $G(j\omega)$ for $\omega \rightarrow \infty$

$$\begin{aligned} G(j\omega) &= C \left(j\omega I - \sum_{k=0}^m A_k e^{-j\omega\tau_k} \right)^{-1} B \\ &= C \left(\frac{I}{j\omega} - \sum_{k=0}^m \frac{A_k e^{-j\omega\tau_k}}{\omega^2} + \mathcal{O}(\omega^{-3}) \right) B, \\ &= \frac{CB}{j\omega} - C \left(\sum_{k=0}^m \frac{A_k e^{-j\omega\tau_k}}{\omega^2} \right) B + \mathcal{O}(\omega^{-3}), \end{aligned}$$

Using this, we can also set up the first terms of the asymptotic expansion of the product of $G(j\omega)$ with its complex conjugate,

$$\begin{aligned} &G(j\omega)^* G(j\omega) \\ &= B^* \left((-j)\omega I - \sum_{k=0}^m A_k^* e^{+j\omega\tau_k} \right)^{-1} C^* C \left(j\omega I - \sum_{k=0}^m A_k e^{-j\omega\tau_k} \right)^{-1} B \\ &= \frac{B^* C^* C B}{\omega^2} - \frac{B^*}{j\omega^3} \left(\sum_{k=0}^m A_k^* C^* e^{+j\omega\tau_k} - \sum_{k=0}^m C A_k e^{-j\omega\tau_k} \right) B + \mathcal{O}(\omega^{-4}), \\ &= \frac{(CB)^* CB}{\omega^2} - \frac{1}{j\omega^3} \left(\sum_{k=0}^m ((CA_k B)^* - CA_k B) \cos(\omega\tau_k) \right. \\ &\quad \left. + j \sum_{k=0}^m ((CA_k B)^* + CA_k B) \sin(\omega\tau_k) \right) + \mathcal{O}(\omega^{-4}), \end{aligned}$$

We now take the trace to obtain the Frobenius norm of $G(j\omega)$. Since the coefficient matrix of the imaginary part is skew-symmetric, it vanishes when

taking the trace. Furthermore, given that matrix $CA_k B$ is real, we obtain

$$\|G(j\omega)\|_F \sim \frac{\|CB\|_F}{\omega^2} - \frac{2}{\omega^3} \sum_{k=1}^m \text{tr}(CA_k B) \sin(\omega\tau_k) + \dots, \quad \omega \rightarrow \infty. \quad (32)$$

We can carry out the same calculation for the approximating transfer function G_N , to find that its Frobenius norm can be asymptotically expanded as

$$\begin{aligned} \|G_N(j\omega)\|_F &\sim \frac{\|CB\|_F}{\omega^2} \\ &- \frac{2}{\omega^3} \sum_{k=1}^m \text{tr}(CA_k B) \Im\{p_N(-\tau_k, j\omega)\} + \dots, \quad \omega \rightarrow \infty. \end{aligned} \quad (33)$$

Now note that the dominant term in both expansions are equal for the two functions. Hence, they exhibit the same asymptotic behaviour.

If N is sufficiently large, then for the ω range that we are interested (namely, beyond the critical ω_T for which the approximation starts breaking down), the term λI will dominate within the inverse expression $(\lambda I - D_N^3)^{-1}$ in the explicit expression (24) for $p_N(t; \lambda)$. Then, it is easily seen that

$$\Im\{p_N(t, j\omega)\} \sim -\frac{1}{\omega} [\ell_1(t) \quad \dots \quad \ell_{N-1}(t)] D_N^b, \quad \omega \rightarrow \infty.$$

that is, it will start to behave as $\mathcal{O}(\omega^{-1})$. This renders the second term in the expansion of $\|G_N(j\omega)\|_F$ of order ω^{-4} rather than of order ω^{-3} , so that the difference E_N between the two Frobenius norms of the transfer functions can in fact be written as

$$\begin{aligned} E_N(\omega) &= \|G_N(j\omega)\|_F - \|G(j\omega)\|_F \\ &= \frac{2}{\omega^3} \sum_{k=1}^m \text{tr}(CA_k B) \sin(\omega\tau_k) + \mathcal{O}(\omega^{-4}). \end{aligned} \quad (34)$$

3.2.3 Error behaviour of γ_N

Using the properties of E_N explained above, we can approximate the error of γ_N as follows

$$\gamma_N^2 - \gamma^2 = \frac{1}{\pi} \int_0^\infty E_N(\omega) d\omega \approx \frac{1}{\pi} \int_{\omega_T(N)}^\infty E_N(\omega) d\omega, \quad (35)$$

that is, neglecting the error for frequencies smaller than $\omega_T(N)$.

Furthermore using the approximation (34) of E_N , based on its asymptotic expansion for $\omega \rightarrow \infty$, we can ultimately describe the error of γ_N as a function of N .

$$\begin{aligned} \gamma_N^2 - \gamma^2 &\approx \frac{1}{\pi} \int_{\omega_T(N)}^\infty \left(\frac{2}{\omega^3} \sum_{k=1}^m \text{tr}(CA_k B) \sin(\omega\tau_k) + \mathcal{O}(\omega^{-4}) \right) d\omega \\ &\approx \frac{2}{\pi} \sum_{k=1}^m \text{tr}(CA_k B) \int_{\omega_T(N)}^\infty \frac{\sin(\omega\tau_k)}{\omega^3} d\omega + \mathcal{O}(\omega_T(N)^{-3}) \\ &\approx \mathcal{O}(N^{-3}). \end{aligned}$$

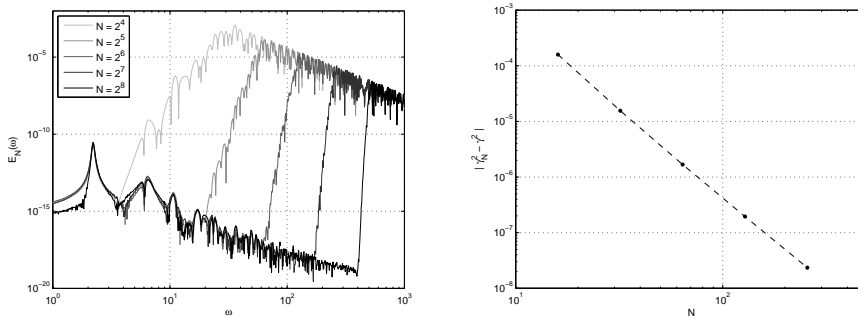


Figure 3: Results for the approximation of the time-delay system of Example 3.5 for $N = 2^p$ with $p = 4, \dots, 8$. Left, error functions E_N of the Frobenius norms of the approximate transfer functions G_N with respect to frequency ω . Right, convergence behaviour in function of N of the errors of the approximate \mathcal{H}_2 norms γ_N corresponding to the E_N functions of the left frame.

In the last step we used our observation that $\omega_T(N)$ is linear in N , and in addition the fact that

$$\int_{a>0}^{\infty} \frac{\sin(\omega\tau_k)}{\omega^3} d\omega = \mathcal{O}(a^{-3}).$$

which can be achieved by using integration by parts.

The errors of E_N and γ_N are illustrated in Figure 3 for Example 3.5. The left frame shows the behaviour of E_N as functions of ω for several N logarithmically distributed between 2^4 and 2^8 , and the right frame plots the resulting errors of the approximate transfer norm approximations γ_N , clearly revealing the expected decline rate.

4 Optimal \mathcal{H}_2 norm synthesis

4.1 Problem formulation

As mentioned in the introduction, we are interested in the case where matrices B , C , and A_k , $k = 0, \dots, m$, depend on a small, fixed number of parameters, say, $p \in \mathbb{R}^{n_p}$. In control applications such parameters typically stem from the presence of a feedback controller with a given structure or order. The set of parameters represents variables of the controller that can be freely chosen, preferably in an optimal way with respect to some desired objective function. In this work we assume that the objective function is expressed by the \mathcal{H}_2 norm of an appropriately defined transfer function. Hence, the corresponding design problem is a *fixed structure optimal \mathcal{H}_2 synthesis problem* (see [16] for the case without delays).

The synthesis problem under consideration can be formulated as

$$\min_p \gamma(p), \tag{36}$$

where $\gamma(p)$ represents the \mathcal{H}_2 norm of

$$G(\lambda; p) = C(p) \left(\lambda I - \sum_{k=0}^m A_k(p) e^{-\lambda \tau_k} \right)^{-1} B(p). \quad (37)$$

Note that, as the \mathcal{H}_2 norm equals infinity for unstable systems, this formulation implicitly requires that p corresponds to a stabilizing controller at the solution.

Since we cannot compute γ exactly, we must resort to an approximation. For this we can use the method as outlined in this chapter. Specifically, we simply fix N to some value, and replace the objective function with the approximation γ_N . So, instead, we solve the problem

$$\min_p \gamma_N(p),$$

with γ_N defined as the \mathcal{H}_2 norm of the discretized system (16) and computed using (20). If we take a large N , the solution will be close to the one of the original problem, but requires more computational effort for computing the objective function evaluations. A way to circumvent this trade-off is to start with a small N to compute a rough estimate of the optimizer, and do some steps with a higher N to have a more accurate value. In this way, the procedure will have cheaper function evaluations, while the end result is as accurate.

4.2 Derivatives

In order to exploit the smoothness of the \mathcal{H}_2 norm, we must of course not only be able to evaluate γ_N , but also to compute its derivatives w.r.t. the controller parameters efficiently.

Our derivations will be based on the fact that, since the system (16) is a standard first-order system, we can use the following general property.

Property 4.1. *Let the symmetric matrices P and Q be the controllability and observability Gramian matrices for the LTI system (16) defined as in Property 2.1. Then the derivatives w.r.t. the system matrices A , B and C are*

$$\frac{\partial(\gamma^2)}{\partial \mathcal{A}_N} = 2P_N Q_N, \quad \frac{\partial(\gamma^2)}{\partial \mathcal{B}_N} = 2\mathcal{B}_N^\top Q_N, \quad \frac{\partial(\gamma^2)}{\partial \mathcal{C}_N} = 2P_N \mathcal{C}_N^\top, \quad (38)$$

where $\partial(\cdot)/\partial M$ denotes the transpose of the matrix containing the entry-wise partial derivatives with respect to matrix M .

Using this property, we will derive expressions for the derivatives w.r.t. the original system matrices in the following theorem. It essentially describes how they can be easily extracted from the derivatives w.r.t. the discretized linear system matrices \mathcal{A}_N , \mathcal{B}_N and \mathcal{C}_N , by making use of their special structure.

Theorem 4.2. *The derivatives of γ_N^2 w.r.t. the original system matrices A_k , $k = 0, \dots, m$ equal*

$$\frac{\partial \gamma_N^2}{\partial A_k} = 2 \left[\ell_1(-\tau_k) I \quad \dots \quad \ell_N(-\tau_k) I \right] P_N Q_N \begin{bmatrix} 0 & \dots & 0 & I \end{bmatrix}^\top, \quad (39)$$

The derivatives w.r.t. the input and output matrices B and C are given by

$$\frac{\partial \gamma_N^2}{\partial B} = 2B^\top q_{NN}, \quad \frac{\partial \gamma_N^2}{\partial C} = 2p_{NN} C^\top, \quad (40)$$

where $p_{NN}, q_{NN} \in \mathbb{R}^{n \times n}$ represent the bottom right block matrices matrices of P_N and of Q_N , defined in (19a)-(19b), respectively.

Proof. We first prove expression (39). The directional derivative of γ_N^2 along ΔA_k equals

$$\begin{aligned} D_{A_k}(\gamma_N^2)[\Delta A_k] &= \lim_{h \rightarrow 0^+} \frac{\gamma_N^2(A_k + h\Delta A_k) - \gamma_N^2(A_k)}{h} \\ &= \text{tr} \left(\frac{\partial(\gamma_N^2)}{\partial A_k} \Delta A_k \right), \end{aligned} \quad (41)$$

which we can expand with the chain rule into

$$\begin{aligned} D_{A_k}(\gamma_N^2)[\Delta A_k] &= D_{\mathcal{A}_N}(\gamma_N^2)[D_{A_k}(\mathcal{A}_N)[\Delta A_k]] \\ &= \text{tr} \left(\frac{\partial(\gamma_N^2)}{\partial \mathcal{A}_N} D_{A_k}(\mathcal{A}_N)[\Delta A_k] \right). \end{aligned}$$

With Property 4.1, this becomes

$$D_{A_k}(\gamma_N^2)[\Delta A_k] = \text{tr}((2P_N Q_N) D_{A_k}(\mathcal{A}_N)[\Delta A_k]). \quad (42)$$

Taking into account that, according to (14), A_k only occurs in the last block row of \mathcal{A}_N , we can directly write that

$$D_{A_k}(\mathcal{A}_N)[\Delta A_k] = [0 \ \cdots \ 0 \ I]^\top \Delta A_k [\ell_1(-\tau_k)I \ \cdots \ \ell_N(-\tau_k)I] \quad (43)$$

Filling in (43) in (42), we arrive at

$$\begin{aligned} D_{A_k}(\gamma_N^2)[\Delta A_k] &= \text{tr} \left((2P_N Q_N) [0 \ \cdots \ 0 \ I]^\top \Delta A_k [\ell_1(-\tau_k)I \ \cdots \ \ell_N(-\tau_k)I] \right) \\ &= \text{tr} \left(\left(2 [\ell_1(-\tau_k)I \ \cdots \ \ell_N(-\tau_k)I] P_N Q_N [0 \ \cdots \ 0 \ I]^\top \right) \Delta A_k \right), \end{aligned}$$

which proves (39) by comparison with (41).

The proof of the derivative expressions with respect to B and C in (40) follows the same line of thought as above. Indeed, by writing out $D_B(\gamma_N^2)[\Delta B]$ as

$$\begin{aligned} D_B(\gamma_N^2)[\Delta B] &= D_{\mathcal{B}_N}(\gamma_N^2)[D_B(\mathcal{B}_N)[\Delta B]] = \text{tr} \left(\frac{\partial(\gamma_N^2)}{\partial \mathcal{B}_N} D_B(\mathcal{B}_N)[\Delta B] \right) \\ &= \text{tr} \left(2B_N^\top Q_N [0 \ \cdots \ 0 \ I]^\top \Delta B \right) \\ &= \text{tr} \left(2B^\top [0 \ \cdots \ 0 \ I] Q_N [0 \ \cdots \ 0 \ I]^\top \Delta B \right) \\ &= \text{tr} \left((2B^\top q_{NN}) \Delta B \right), \end{aligned}$$

and similarly for $\gamma_N^2(C)[\Delta C]$, conjecture (40) follows by comparison, concluding the proof. \square

Once the partial derivatives with respect to A_k , B and C have been established, the derivatives w.r.t. the (controller) parameters p can be easily attained via the chain rule.

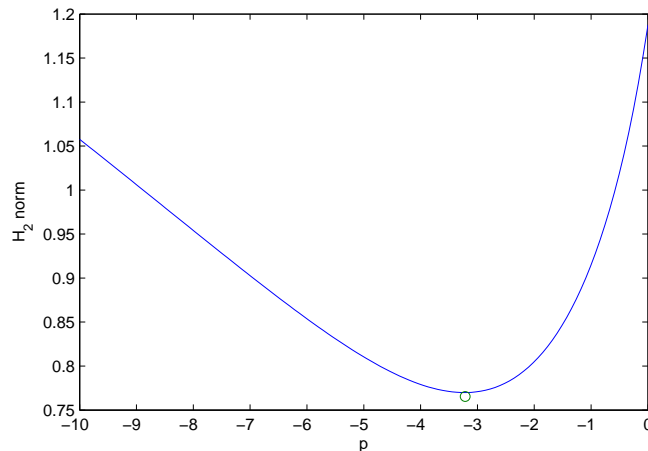


Figure 4: Evolution of the exact ($N = \infty$) \mathcal{H}_2 norm of the scalar example outlined in Subsection 5.1. The optimum, computed by a spectral approximation of this system with discretization parameter $N = 6$, is indicated by a ‘o’.

5 Numerical examples

5.1 Scalar example

We reuse the example data of Example 3.5, except that we now introduce a scalar parameter p in the topleft entry of A_0 ,

$$A_0 = \begin{bmatrix} p & 1 \\ -4 & -1 \end{bmatrix}.$$

Fixing the discretization parameter to $N = 6$, we optimize the approximate \mathcal{H}_2 norm. The resulting approximated optimum is indicated in Figure 4 by a small circle. The blue line shows the evolution of the exact \mathcal{H}_2 norm (computed with a much larger N) for values of $p \in [-10, 0]$. It is seen that, even for a low discretization level, the approximation of the optimum is already quite good. Indeed, the absolute error between the optimal value of p and corresponding optimal value of the objective function for $N = 6$ and for $N \gg 6$ was equal to approximately $3\mathbf{e}-3$ and $8\mathbf{e}-4$ respectively.

Should we want to acquire a higher accuracy, then we can increase the number of discretization points, and perform the optimization procedure once again. If the hot-start minimizer from the previous run is used, the number of iterations needed to converge is expected to be low.

5.2 Heat transfer system from [20]

In [20], a water-based heating system is introduced. The equations that model this heat transfer process read as follows:

$$\begin{cases} T_h x'_h(t) = -x_h(t - \eta_h) + K_b x_a(t - \tau_b) + K_u x_{h,set}(t - \tau_u), \\ T_a x'_a(t) = -x_a(t) + x_c(t - \tau_e) + K_a (x_h(t) - \frac{1+q}{2} x_a(t) - \frac{1-q}{2} x_c(t - \tau_e)), \\ T_d x'_d(t) = -x_d(t) + K_d x_a(t - \tau_d), \\ T_c x'_c(t) = -x_c(t - \eta_c) + K_c x_d(t - \tau_c), \\ x'_e(t) = -x_c(t) + x_{c,set}(t), \end{cases} \quad (44)$$

where the x -variables denote the temperature measured at different places in the circuit. For the values of the parameters, see [20, §5.1]. The set-point value $x_{h,set}(t)$ is determined by the static state feedback controller

$$x_{h,set}(t) = p^\top [x_h(t) \quad x_a(t) \quad x_d(t) \quad x_c(t) \quad x_e(t)]^\top.$$

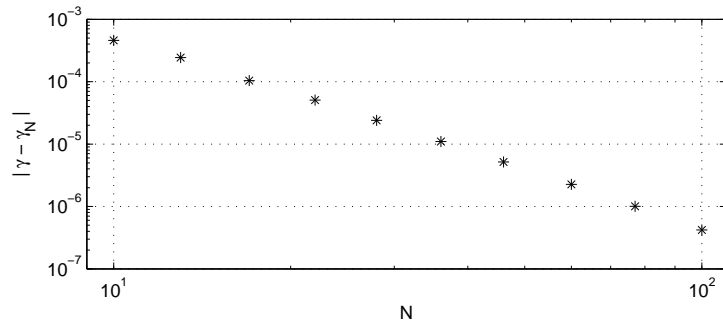
We now optimize the \mathcal{H}_2 norm for this system, where we consider the transfer function from the last state to the last state, i.e., $B^\top = C = [0 \ 0 \ 0 \ 0 \ 1]$. As starting point for the optimization process, we choose the stable controller that resulted from the spectral abscissa minimization with the approach presented in [19]. Let us however first investigate a suitable N . Figure 5(a) shows the errors of the \mathcal{H}_2 norm for 10 values of N logarithmically distributed between 10 and 100 (the error was determined with respect to $N = 200$). Note that we indeed observe the polynomial decrease as discussed in Section 3.2. Based on this figure, we choose $N = 70$.

The \mathcal{H}_2 norm at the initial point is equal to 8.78371. We now use the BFGS method to minimize this value. Because the computation time of an evaluation heavily depends on N , we first do a preliminary optimization run with a smaller N . In Figure 5(a), we see that for $N = 10$ already a reasonable approximation accuracy is achieved. We therefore first optimize with this smaller value of N in order to find a starting point that is already close to the solution for the optimization with $N = 70$. We were able to decrease the value of the \mathcal{H}_2 norm to 7.51619. The optimal controller parameters are $p^\top = [1.0560 \ 9.9391 \ 10.866 \ 12.612 \ -0.79074]$. Figure 5(b) shows the spectrum of resulting controller with a minimal spectral abscissa and with a minimal \mathcal{H}_2 norm.

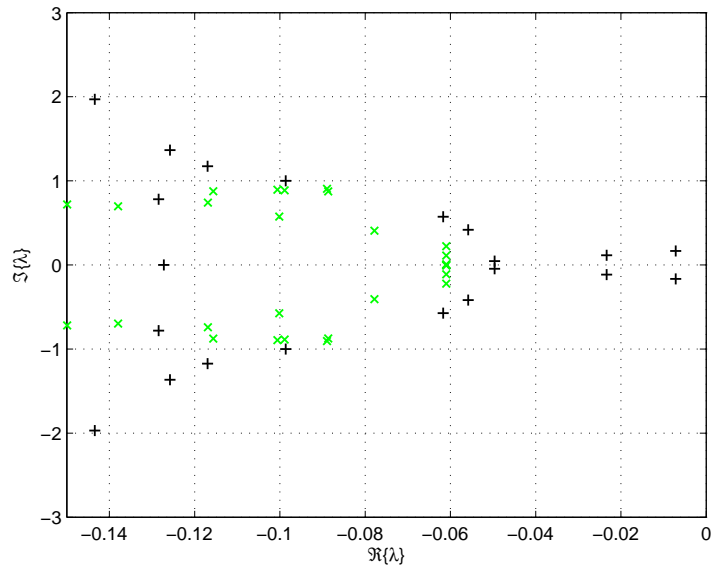
Note that the characteristic roots are more spread out in the complex plane and thus less susceptible to disturbances or perturbations, indicating the lower \mathcal{H}_2 norm. However, since the spectral abscissa is no longer minimal, the right-most characteristic roots are closer to the imaginary axis. This illustrates the inherent trade-off between performance and robustness.

5.3 Updated heat transfer example from [14]

The next example is an updated, larger model for the same experimental heat-transfer setup, as presented in [14]. Now, the time-delay system has a dimension of 11 and there are 6 delays appearing. The parameters p for this example again stem from a static state feedback controller. More precisely, the system



(a) Absolute errors of the approximated value γ_N as approximation to γ for several values of N .



(b) Comparison of the spectra minimized with respect to the spectral abscissa (green \times) and with respect to the \mathcal{H}_2 norm (+).

Figure 5: Results for the \mathcal{H}_2 norm optimization of the heat transfer system from [20]

is described by

$$x'(t) = \sum_{k=0}^6 A_k(p)x(t - \tau_k) + Bw(t) \quad (45)$$

$$z(t) = Cx(t) \quad (46)$$

where the delays satisfy

$$\tau_1 = 3, \quad \tau_2 = 5, \quad \tau_3 = 7, \quad \tau_4 = 15, \quad \tau_5 = 23, \quad \tau_6 = 29.$$

The entries of the system matrices $A_0, A_1, A_2, A_4, A_5, A_6$ are equal to zero except for the entries

$$\begin{aligned} A_0(1,1) &= -1/5, & A_0(4,3) &= 0.575/3, & A_1(5,4) &= 0.975/5, \\ A_0(2,2) &= -1/25, & A_0(4,4) &= -1.425/3, & A_2(3,2) &= 0.983/5, \\ A_0(3,3) &= -1/5, & A_0(4,7) &= 0.425/3, & A_2(6,5) &= 0.9/17, \\ A_0(5,5) &= -1/5, & A_0(4,8) &= 0.425/3, & A_2(9,8) &= 0.97/5, \\ A_0(6,6) &= -1/17, & A_0(8,3) &= 0.425/3, & A_2(10,9) &= 0.92/5, \\ A_0(9,9) &= -1/5, & A_0(8,4) &= 0.425/3, & A_4(1,6) &= 0.973/5, \\ A_0(10,10) &= -1/15, & A_0(8,7) &= 0.575/3, & A_5(2,1) &= 0.96/25, \\ A_0(11,10) &= -1, & A_0(8,8) &= -1.425/3, & A_6(7,7) &= -1/63. \end{aligned}$$

Matrix A_3 stems from a static feedback control law,

$$A_3 = -[0 \ 0 \ 0 \ 0 \ 0 \ 0 \ 1/63 \ 0 \ 0 \ 0 \ 0]^\top [p(1) \ \dots \ p(11)].$$

As for the input and output matrices, we take

$$B = [0 \ \dots \ 0 \ 0.042/15 \ 1]^\top, \quad C = \begin{bmatrix} 0 & \dots & 0 & 1 & 0 \\ 0 & \dots & 0 & 0 & 1 \end{bmatrix},$$

meaning that we take one input acting on the two last states, which are also the two outputs.

In [14], four stabilizing feedback controllers were synthesized, the first by minimizing the spectral abscissa according to the method of [19], and the other three by additionally placing poles at specific points in the complex plane.

We choose $N = 20$ and perform a minimization of the \mathcal{H}_2 norm starting from these four stable points. The resulting optimal K values are listed in Table 1. We see that for the four initial values, K converges to the same optimizer. The corresponding minimal \mathcal{H}_2 norm for each of these K was equal to 5.1960, and the spectrum of characteristic roots is shown in Figure 6.

6 Conclusions

We have proposed a numerical approach to compute the \mathcal{H}_2 norm for time-delay systems of the retarded type with fixed delays. The method is based on a spectral discretization of the delay interval, which results in a larger system without delays that approximates the original time-delay system. The convergence behaviour as a function of a discretization parameter N has been analyzed, and assures a decline rate of $\mathcal{O}(N^{-3})$. The computation of derivatives has also been discussed. Furthermore, the use of this approach in the framework of optimal \mathcal{H}_2 control design has been demonstrated.

$p_0 =$	p_{SN1}	p_{SN2}	K_{SN3}	p_{SN4}
$\gamma(p_0)$	6.71476	8.00088	7.13777	7.95949
$p^*(1)$	-4.6646e+01	-4.6653e+01	-4.6646e+01	-4.6666e+01
$p^*(2)$	1.7831e+02	1.7832e+02	1.7832e+02	1.7835e+02
$p^*(3)$	-2.0467e+03	-2.0467e+03	-2.0467e+03	-2.0467e+03
$p^*(4)$	1.6122e+04	1.6121e+04	1.6122e+04	1.6121e+04
$p^*(5)$	-7.9448e+02	-7.9446e+02	-7.9449e+02	-7.9435e+02
$p^*(6)$	-1.1955e+03	-1.1954e+03	-1.1955e+03	-1.1951e+03
$p^*(7)$	3.6946e+02	3.6945e+02	3.6946e+02	3.6944e+02
$p^*(8)$	-1.3989e+04	-1.3989e+04	-1.3989e+04	-1.3988e+04
$p^*(9)$	5.9998e+02	5.9996e+02	5.9998e+02	5.9987e+02
$p^*(10)$	1.2374e+03	1.2374e+03	1.2374e+03	1.2371e+03
$p^*(11)$	-2.2728e+01	-2.2728e+01	-2.2728e+01	-2.2729e+01

Table 1: Optimal parameter values p^* resulting from the minimization of the \mathcal{H}_2 norm started from starting points SN1, \dots , SN4 (parameter values for these points can be found in [14]).

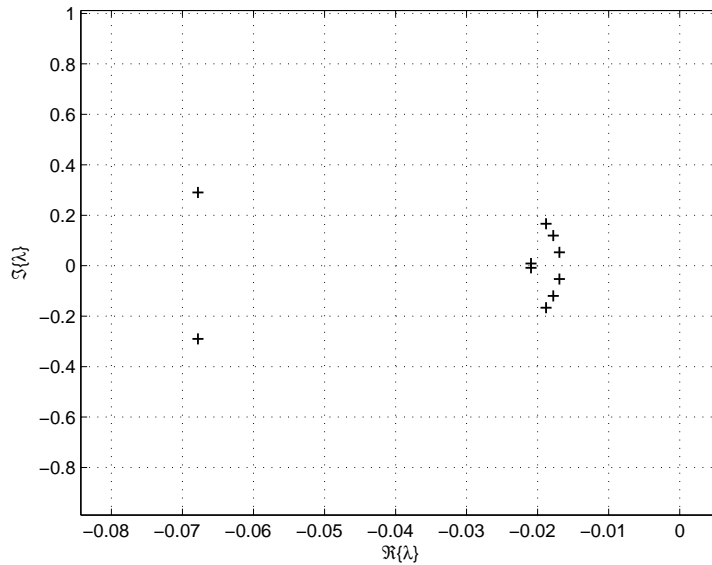


Figure 6: Spectrum of the heat transfer model from [14] after minimization of the \mathcal{H}_2 norm .

Acknowledgements

This article presents results of the Belgian Programme on Interuniversity Poles of Attraction, initiated by the Belgian State, Prime Minister's Office for Science, Technology and Culture, the Optimization in Engineering Centre OPTEC, and the project STRT1-09/33 of the K.U.Leuven Research Foundation.

A Appendix: proof of Theorem 3.4

Proof. Let us start with writing G_N as

$$G_N(\lambda) = \mathcal{C}_N(\lambda I - \mathcal{A}_N)^{-1} \mathcal{B}_N \\ = C \begin{bmatrix} 0 & \cdots & 0 & I_n \end{bmatrix} \frac{\text{adj}(\lambda I - \mathcal{A}_N)}{\det(\lambda I - \mathcal{A}_N)} \begin{bmatrix} 0 & \cdots & 0 & I_n \end{bmatrix}^\top B, \quad (47)$$

where $\text{adj}(\cdot)$ denotes the adjugate of a matrix. By partitioning the matrix \mathcal{A}_N into the following 2x2 block matrix

$$\mathcal{A}_N = \left[\begin{array}{c|c} D_N^a \otimes I_n & D_N^b \otimes I_n \\ \hline a_{N1} \cdots a_{NN-1} & a_{NN} \end{array} \right],$$

we can write down the denominator based on the formula for the determinant of a two-by-two block matrix involving the Schur complement

$$\det(\lambda I - \mathcal{A}_N) = \det(\lambda I - (D_N^a \otimes I_n)) \\ \det \left((\lambda I_n - a_{NN}) - [a_{N1} \cdots a_{NN-1}] \left[\lambda I - (D_N^a \otimes I_n) \right]^{-1} [D_N^b \otimes I_n] \right) \\ = \det((\lambda I - D_N^a) \otimes I_n) \\ \det \left(\lambda I_n - a_{NN} - [a_{N1} \cdots a_{NN-1}] \left[(\lambda I - D_N^a)^{-1} D_N^b \right] \otimes I_n \right).$$

Using (29) and (27) of Theorem 3.2 and further on substituting the a_{Nj} , $j = 1, \dots, N$ according to (14), we can simplify this further into

$$\det(\lambda I - \mathcal{A}_N) \\ = \det(\lambda I - D_N^a)^n \det \left(\lambda I_n - a_{NN} - [a_{N1} \cdots a_{NN-1}] \begin{bmatrix} p_N(\theta_1; \lambda) I_n \\ \vdots \\ p_N(\theta_{N-1}; \lambda) I_n \end{bmatrix} \right) \\ = s(\lambda)^n \det \left(\lambda I_n - \sum_{j=1}^N a_{Nj} p_N(\theta_j; \lambda) \right) \\ = s(\lambda)^n \det \left(\lambda I_n - \sum_{j=1}^N \left(\sum_{k=0}^m \ell_j(-\tau_k) A_k \right) p_N(\theta_j; \lambda) \right) \\ = s(\lambda)^n \det \left(\lambda I_n - \sum_{k=0}^m A_k \left(\sum_{j=1}^N \ell_j(-\tau_k) p_N(\theta_j; \lambda) \right) \right) \\ = s(\lambda)^n \det \left(\lambda I_n - \sum_{k=0}^m A_k p_N(-\tau_k; \lambda) \right). \quad (48)$$

For the nominator of (47), let us introduce $\Delta(\lambda)$ as a short-hand notation for the n -by- n matrix

$$\Delta(\lambda) = \begin{bmatrix} 0 & \cdots & 0 & I_n \end{bmatrix} \text{adj}(\lambda I - \mathcal{A}_N) \begin{bmatrix} 0 & \cdots & 0 & I_n \end{bmatrix}^\top.$$

Following the same reasoning based on Schur complements, we can write out the (μ, ν) -th element of $\Delta(\lambda)$ as

$$\begin{aligned} \Delta_{\mu, \nu}(\lambda) &= \det((\lambda I - D_N^a) \otimes I_n) \\ &\quad \det \left((\lambda \tilde{I}_n - \tilde{a}_{NN}) - [\tilde{a}_{N1} \ \cdots \ \tilde{a}_{NN-1}] [(\lambda I - D_N^a) \otimes I_n]^{-1} [D_N^b \otimes \tilde{I}_n] \right), \end{aligned}$$

where the subscript \sim indicates that the appropriate row and/or column have been removed with respect to μ and ν . Rearranging terms as before and again using Theorem 3.2 gives

$$\begin{aligned} \Delta_{\mu, \nu}(\lambda) &= s(\lambda)^n \det \left(\lambda \tilde{I}_n - \begin{bmatrix} \tilde{a}_{N1} & \cdots & \tilde{a}_{NN} \end{bmatrix} \begin{bmatrix} p_N(\theta_1; \lambda) \tilde{I}_n \\ \vdots \\ p_N(\theta_N; \lambda) \tilde{I}_n \end{bmatrix} \right) \\ &= s(\lambda)^n \det \left(\lambda \tilde{I}_n - \sum_{j=1}^N \tilde{a}_{Nj} \tilde{I}_n p_N(\theta_j; \lambda) \right) \\ &= s(\lambda)^n \det \left(\lambda \tilde{I}_n - \sum_{k=0}^m \tilde{A}_k p_N(-\tau_k; \lambda) \right), \end{aligned}$$

which, being true for every μ and ν , implies that

$$\Delta(\lambda) = s(\lambda)^n \text{adj} \left(\lambda I_n - \sum_{k=0}^m A_k p_N(-\tau_k; \lambda) \right). \quad (49)$$

With (48) and (49) substituted in (47), we can derive the proposition

$$\begin{aligned} G_N(\lambda) &= \frac{C \Delta(\lambda) B}{\det(\lambda I - \mathcal{A}_N)} = C \frac{\text{adj} \left(\lambda I_n - \sum_{k=0}^m A_k p_N(-\tau_k; \lambda) \right)}{\det \left(\lambda I_n - \sum_{k=0}^m A_k p_N(-\tau_k; \lambda) \right)} B \\ &= C \left(\lambda I_n - \sum_{k=0}^m A_k p_N(-\tau_k; \lambda) \right)^{-1} B \\ &= \hat{G}_N(\lambda), \end{aligned}$$

thereby concluding the proof. \square

References

- [1] R. Bartels and G. Stewart. Solution of the matrix equation $AX + XB = C$. *Comm. A.C.M.*, 15(9):820–826, 1972.
- [2] A. Bellen and S. Maset. Numerical solution of constant coefficient linear delay differential equations as abstract Cauchy problems. *Numer. Math.*, 84(3):351–374, 2000.

- [3] P. Benner, J.-R. Li, and T. Penzl. Numerical solution of large-scale Lyapunov equations, Riccati equations, and linear-quadratic optimal control problems. *Numer. linear Algebr.*, 15:755B–777, 2008.
- [4] J.-P. Berrut and L. N. Trefethen. Barycentric Lagrange interpolation. *SIAM Rev.*, 46(3):501–517, 2004.
- [5] D. Breda, S. Maset, and R. Vermiglio. Pseudospectral differencing methods for characteristic roots of delay differential equations. *SIAM J. Sci. Comput.*, 27(2):482–495, 2005.
- [6] D. Breda, S. Maset, and R. Vermiglio. Pseudospectral differencing methods for characteristic roots of delay differential equations. *SIAM J. Sci. Comput.*, 27(2):482–495, 2005.
- [7] R. F. Curtain and H. Zwart. *An introduction to infinite-dimensional linear systems theory*. Springer-Verlag, NY, 1995.
- [8] J. Doyle, K. Glover, P. P. Khargonekar, and B. Francis. State-space solutions to standard \mathcal{H}_2 and \mathcal{H}_∞ control problems. *IEEE Trans. Autom. Control*, 34(8):831–847, 1989.
- [9] J. Hale and S. M. Verduyn Lunel. *Introduction to functional differential equations*. Springer-Verlag, 1993.
- [10] S. Hammarling. Numerical solution of the stable, non-negative definite Lyapunov equation. *IMA J. Numer. Anal.*, 2:303–323, 1982.
- [11] I. M. Jaimoukha and E. M. Kasenally. Krylov subspace methods for solving large Lyapunov equations. *SIAM J. Numer. Anal.*, 31(1):227–251, 1994.
- [12] E. Jarlebring, J. Vanbiervliet, and W. Michiels. Characterizing and computing the \mathcal{H}_2 norm of time-delay systems by solving the delay Lyapunov equation. Technical Report 553, K.U.Leuven, Leuven, Belgium, 2009. Submitted.
- [13] W. Michiels and S.-I. Niculescu. *Stability and Stabilization of Time-Delay Systems: An Eigenvalue-Based Approach*. Advances in Design and Control 12. SIAM Publications, Philadelphia, 2007.
- [14] W. Michiels, T. Vyhlídal, and P. Zítek. Control design for time-delay systems based on quasi-direct pole placement. *Journal of Process Control*, 20(3):337–343, 2010.
- [15] S.-I. Niculescu. *Delay effects on stability. A robust control approach*. Springer-Verlag London, 2001.
- [16] D. Noll, J.-B. Thevenet, P. Apkarian, and H.D. Tuan. A spectral quadratic sdp method with applications to fixed-order H_2 and H_∞ synthesis. *European Journal of Control*, 10(6):527–538, 2004.
- [17] J.-P. Richard. Time-delay systems: an overview of some recent advances and open problems. *Automatica*, 39(10):1667–1694, 2003.

- [18] V. Simoncini. A new iterative method for solving large-scale Lyapunov matrix equations. *SIAM J. Sci. Comput.*, 29(3):1268–1288, 2007.
- [19] J. Vanbiervliet, K. Verheyden, W. Michiels, and S. Vandewalle. A non-smooth optimisation approach for the stabilisation of time-delay systems. *ESAIM: Control, Optimisation and Calculus of Variations*, 14(3):478–493, 2008.
- [20] T. Vyhřídál. *Analysis and synthesis of time delay system spectrum*. PhD thesis, Department of Mechanical Engineering, Czech Technical University in Prague, 2003. Text available from http://www.cak.fs.cvut.cz/Dokumenty/thesis_tomas.pdf.
- [21] Kemin Zhou, John C. Doyle, and Keith Glover. *Robust and optimal control*. Prentice-Hall, Inc., Upper Saddle River, NJ, USA, 1996.